Gradient Pattern Analysis of Cosmic Structure Formation: Norm and Phase Statistics

A.P.A. Andrade [1], A.L. B. Ribeiro [2] & R.R. Rosa [3]

1,2 - Laboratório de Astrofísica Teórica e Observacional, Departamento de Ciências Exatas e Tecnológicas, Universidade Estadual de Santa Cruz, Rodovia Ilhéus-Itabuna km 16, 45662.000, Ilhéus, Brasil.

3 - Laboratório Associado de Computação e Matemática Aplicada, Instituto Nacional de Pesquisas Espaciais, 12201-970, São José dos Campos, Brasil.

Abstract

This paper presents the preliminary results of the characterization of pattern evolution in the process of cosmic structure formation. We are applying on N-body cosmological simulations data the technique proposed by Rosa, Sharma & Valdivia (1999) and Ramos et al. (2000) to estimate the time behavior of asymmetries in the gradient field. The gradient pattern analysis is a well tested tool, used to build asymmetrical fragmentation parameters estimated over a gradient field of an image matrix able to quantify a complexity measure of nonlinear extended systems. In this investigation we work with the high resolution cosmological data simulated by the Virgo consortium, in different time steps, in order to obtain a diagnostic of the spatio-temporal disorder in the matter density field. We perform the calculations of the gradient vectors statistics, such as mean, variance, skewness, kurtosis, and correlations on the gradient field. Our main goal is to determine different dynamical regimes through the analysis of complex patterns arising from the evolutionary process of structure formation. The results show that the gradient pattern technique, specially the statistical analysis of second and third gradient moment, may represent a very useful tool to describe the matter clustering in the Universe.

Key words: pattern formation, gradient moments, cosmic structure formation
PACS:

[1] apaula@uesc.br
[2] albr@uesc.br
[3] reinaldo@lac.inpe.br

1 Introduction

Understanding how the spatio-temporal organization of matter happens in the Universe is an important task in modern science. The standard model for cosmic structure formation considers the existence of small inhomogeneities in the matter density field which grew up, in an isotropically expanding universe, trough gravitational clustering. As the fluctuation become intensified, they start to interact which other performing a highly nonlinear evolution during the matter clustering, leading to a cosmic matter distribution settles into an anisotropic patterns. In this dynamical regime, phase coupling can not be avoided, and we can expect a nontrivial asymmetrical pattern arising as the system evolves to a highly inhomogeneous field, being composed by galaxies accumulated in walls, filaments and dense compact clusters, interlocked by large voids regions, characterizing a *foamlike appearance* in the cosmic matter distribution (Weygaert, 2002). Over the nonlinear regime, N-body simulations are used to follow the later evolution of the matter content in the Universe, which is dominated by weakly interacting particles, being the gravity the main interacting force, but also considering corrections factors for dissipational physical effects and hydrodynamical processes (Springel et al., 2005).

The main tools used in cosmology to investigate the evolutionary process of structure formation and compare theoretical models with observations are statistical (Martinez & Saars, 2002). Usually, they are based on a spatial statistics (global mean-field) or a local (nearest-neighbor) analysis. The most popular tools used to describe the large scale structures are the spatial statistics such as the Fourier analysis and the N-point correlation function (e.g. Bardeen et al., 1986). However, other clustering measure, like the local statistics, are being extensively used to provide complementary information to the spatial statistics. They include the topological investigation of the density field, such as the nearest neighbor statistics, the genus and the Minkowski functional (e.g. Mecke, Buchert & Wagner, 1994); the stochastic geometry analysis, which provides a geometrical model of the cellular distribution of matter in the Universe (Bernardeau & Weygaert, 1996; Weygaert, 2002); and the phase mapping analysis used to describe phase patterns in Fourier space (Chiang, Coles & Naselsky, 2002). All these tools complement each other in the investigation of cosmic structure formation and evolution. The purpose of this paper, is to test the ability of the *gradient pattern analysis* (GPA) technique to help the investigation of the spatial-temporal organization of matter in the Universe. We hope this new approach may represent a simple and useful tool to investigate the cosmic structure clustering, as well to compare structural theoretical predictions with observations, since the GPA is a very sensitive technique and, in contrast with other nearest-neighbor methods, does not require large number of points. Actually, GPA has been used to characterize spatial structures

from the point of view of their irregularities meanwhile most the techniques are based on the presence of regularities.

The GPA technique was proposed by Rosa, Sharma & Valdivia (1999), in order to characterize and quantify pattern formation and evolution in complex systems. The measures obtained by GPA is based on the spatio-temporal local density amplitude fluctuations on a structure represented as a dynamical gradient pattern, which may characterize nonlinear emergence and evolution of ordered structures from a random initial condition. This technique has being successfully applied to several nonlinear problems in physics, chemistry and biology fields, being able to characterize symmetry breaks, extended pattern evolution, as well the spatio-temporal relaxation in complex systems (Rosa et al., 2003 and references there in). At this moment, the GPA technique is also being applying on topological feature investigation in the cosmic microwave background maps (Rosa et al., 2006). In this work, we give a particular attention to the investigation of the second and third gradient moments to describe the pattern formation and evolution of cosmic structure formation in a two-dimensional mesh. For this purpose, we perform the statistical analysis of norms and phases of the gradient vectors for the particle density field in N-Body simulations. We estimate mean, variance, skewness, kurtosis and correlations between the gradient vectors. In order to explore symmetries break, we have extended the calculation for both asymmetric and the whole gradient field.

2 The Gradient Pattern Analysis

If we consider spatial extended systems in two dimensions (x,y) their amplitude distribution can be represented as an envelope A(x,y), which can be approximated by a square matrix of amplitude $\mathbf{A} = \{a_{m,m}\}$, in which the two dimensions, x and y, are discretized into M x M pixels. Thus, a dynamical sequence of N matrices is related to a temporal evolution of a visualized envelope A(x,y,t). The spatial fluctuation of the global pattern A(x,y) can be represented by its gradient vector field $G_t = \nabla[A(x,y)]_t$. The local spatial fluctuations, between a pair of neighbor cells, of the global pattern is characterized by its gradient vector at corresponding mesh-points in two dimensional space. In this representation, the relative values between cells ($\Delta A \equiv |A(i,j) - A(i+1,j+1)|$) are dynamically relevant, rather than the pixels absolute values. Indeed, in a gradient field such relatives values, ΔA, can be characterized by each local vector norm ($r_{i,j}$) and phase ($\phi_{i,j}$). Thus a given scalar field can be represented by a gradient field for the local amplitude fluctuations, and its gradient pattern can be represented by a pair of matrices, one for norms and other for phases. Indeed, a natural representation is by means of a complex matrix, where each element corresponds to a respective

complex number $z_{i,j}$ representing each vector from the gradient pattern. Thus, a given matricial scalar field can be represented as a composition of four gradient moments (Rosa et al., 2003: first order, g_1, is the global representation of the vectors distribution; second order, g_2, is the global representation of norms; the third, g_3, is the global representation of phases; and fourth order, g_4, the global complex representation of the gradient pattern. In this work, we are focusing on the second and third gradient moments.

2.1 The First Gradient Moment

A possible information that we can extract from the distribution of the gradient vector field is about symmetry breaking between pairs of vectors. Let us consider two vectors V_i and V_j, with $i \neq j$ belonging to the G_t field. We could say that V_i and V_j are vectorially symmetric if $V_i = -V_j$, so that $R_{i,j} = V_i - V_j = 0$. In computer terms, we could say that the resulting vector, $R_{i,j}$, is null within a tolerance ϵ. The ϵ value would be established according to distribution of the gradient vectors, e.g., equal to one tenth of: (a) standard deviation of magnitudes, and (b) misalignment between them (Rosa, Sharma & Valdivia, 1998). If we remove every pair of symmetric vectors from the G_t field, we will be generating a field with L vectors, all of them vectorially asymmetric. The parameter L would be a first measure of asymmetries in the gradient field. For the asymmetrical vector set, we could also try to perform a statistical analysis of norms and phases. In Figure 1 we present the complete schematic representation of the Gradient Pattern Analysis of a bi-dimensional scalar matricial field. It is also possible to extend the same approach for a data set in three dimensions (x,y,z), building an amplitude matrix A(x,y,z,t), similarly $\mathbf{A} = \{a_{m,m,m}\}$ and a three-dimensional gradient field $G_t = \nabla[A(x,y,z)]_t$.

2.2 The Second and Third Gradient Moment

For the second and third moments, there is no formal computational operation to calculate them in literature. However, to extract basic information about amplitudes and orientation distribution of the gradient field vectors, it is possible to perform a basic statistical analysis between vectors by the norms ($r_{i,j}$) and phases ($\phi_{i,j}$) matrix. This statistical analysis could include:

- mean: $\langle r_{i,j} \rangle$ and $\langle \phi_{i,j} \rangle$;
- variance: $\langle (r_{i,j} - \langle r_{i,j} \rangle)^2 \rangle$ and $\langle (\phi_{i,j} - \langle \phi_{i,j} \rangle)^2 \rangle$;
- skewness: $\frac{\left\langle (r_{i,j} - \langle r_{i,j} \rangle)^3 \right\rangle}{\langle (r_{i,j} - \langle r_{i,j} \rangle)^2 \rangle^{\frac{3}{2}}}$ and $\frac{\left\langle (\phi_{i,j} - \langle \phi_{i,j} \rangle)^3 \right\rangle}{\langle (\phi_{i,j} - \langle \phi_{i,j} \rangle)^2 \rangle^{\frac{3}{2}}}$;

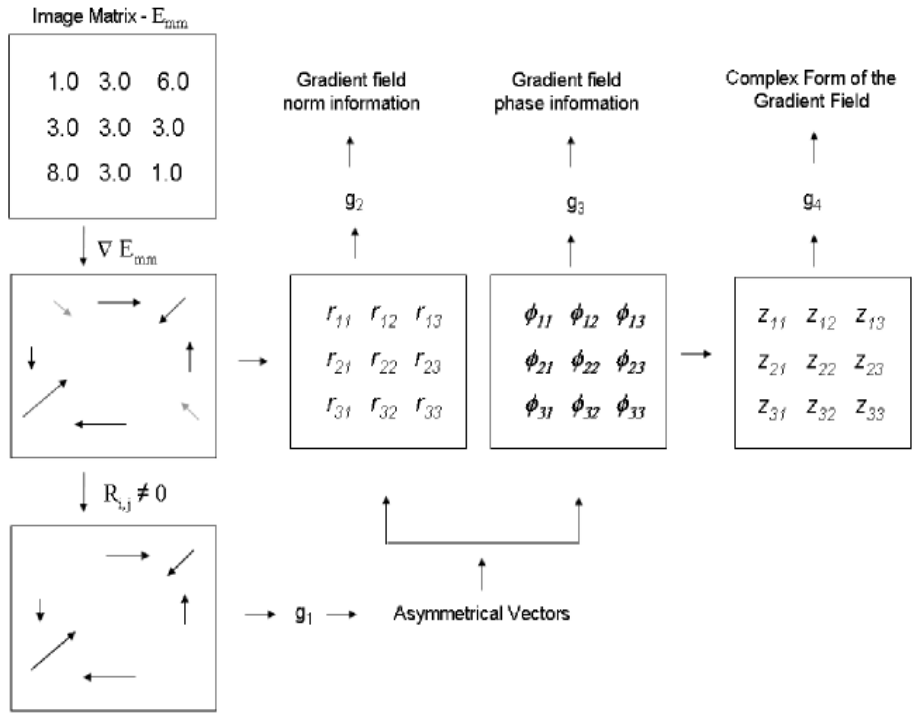

Fig. 1. GPA Summry: building the gradient moments from an image scale matrix

- kurtosis: $\frac{\left\langle (r_{i,j}-\langle r_{i,j}\rangle)^4 \right\rangle}{\langle (r_{i,j}-\langle r_{i,j}\rangle)^2\rangle^2}$ and $\frac{\left\langle (\phi_{i,j}-\langle \phi_{i,j}\rangle)^4 \right\rangle}{\langle (\phi_{i,j}-\langle \phi_{i,j}\rangle)^2\rangle^2}$;
- complex correlation: $\langle z_{i,j} z_{l,m} \rangle$.

3 Data Base and Analysis

For the first check of GPA ability in the process of cosmic structure formation, we have chosen to perform the analysis only in a two-dimensional mesh estimated over the public domain high resolution N-body cosmological data simulated by the *Virgo Consortium (http://www.mpa-garching.mpg.de/Virgo/)* for a Λ-CDM Universe (Jenkins et al., 1998). To assure a good statistical assembly, we have computed 150 bi-dimensional amplitude matrix for the density field, E_{mn} , in seventeen time step (redshift, z) on interval $(0 \leq z \leq 10)$, computed in a mesh grid of (180×180), estimated over a simulated volume of $(120 \times 120 \times 10)h^{-3}Mpc^3$. This discretized mesh enable us to deal with local amplitude fluctuations with resolution of $\sim 0.7Mpc\ h^{-1}$, scale in which we can map organizing substructures inside galaxy clusters. In Figure 2, we present three of this bi-dimensional slices of the simulated volume for three redshift values: z = 10, 3 and 0. Also in Figure 2, we show the frames of

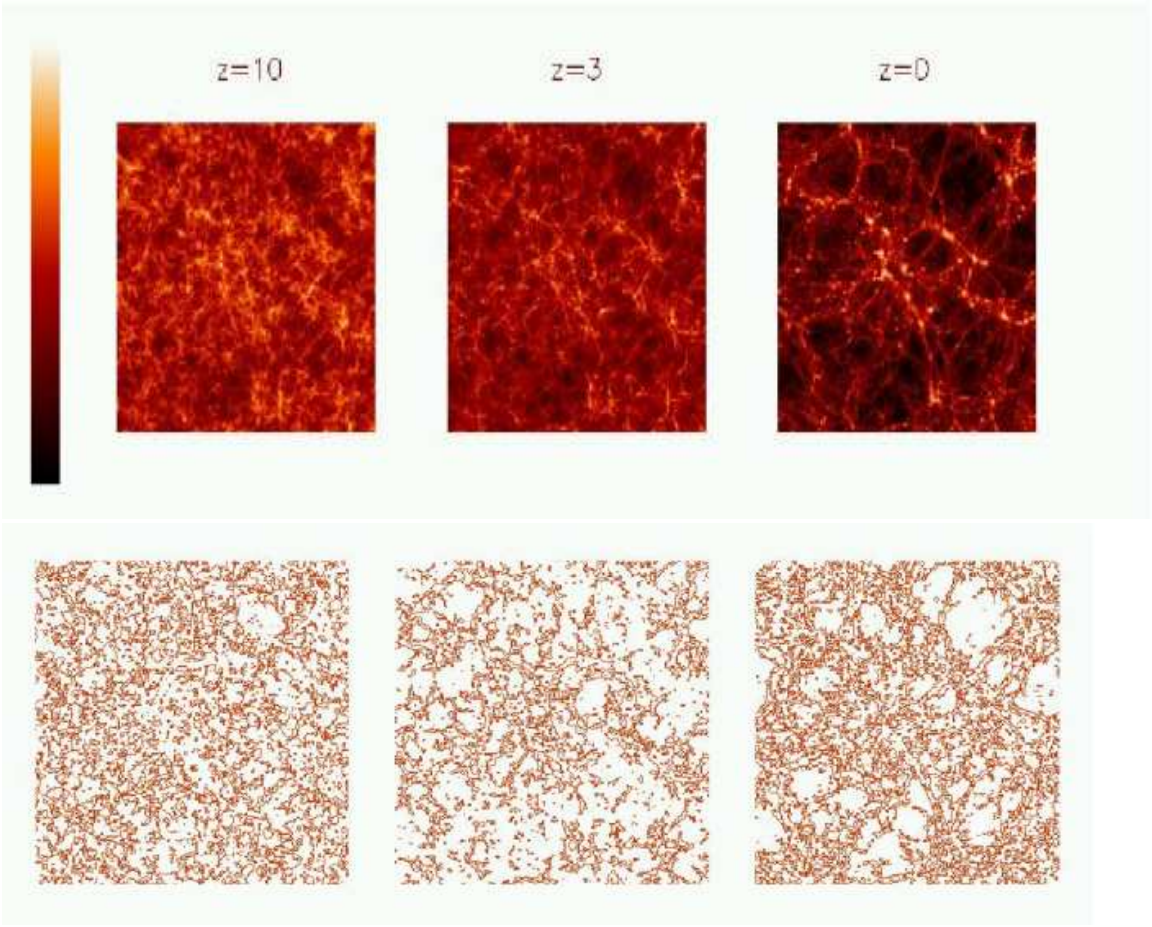

Fig. 2. Three slices of a tri-dimensional N-body simulations for a Λ-CDM universe on redshifts: 10, 3 and 0. The frames on the bottom are their respective intensity contours plot.

their respective intensity contours plot. The matter organization in clusters, filaments and voids is clearly seen in this frames. Remembering that higher redshift represents earlier epochs, while the redshift zero is the present time.

In order to test the efficiency of the GPA technique to characterize pattern evolution in process of structure formation, we have performed a detailed statistical analysis between norms and phases, the second and third gradient moments of the gradient field. We have worked with every 150 volume slices for each one of the seventeen redshift intervals simulated. In the final analysis we have performed the mean value between the 150 slices to compute the statistical moment. We have considered independently the analysis in two cases: first, for all the vectors in the gradient field and second, only for the asymmetrical vectors estimated in the gradient field, as discussed in section 2.1. We also have performed a simulation of eighteen set of 150 random matrices, with mean amplitude in the same interval as the N-body data, in order to compare the statistical analysis of the norms and phase vectors with a random distribution. The main results obtained are illustrated in Figures 3, 4 and 5.

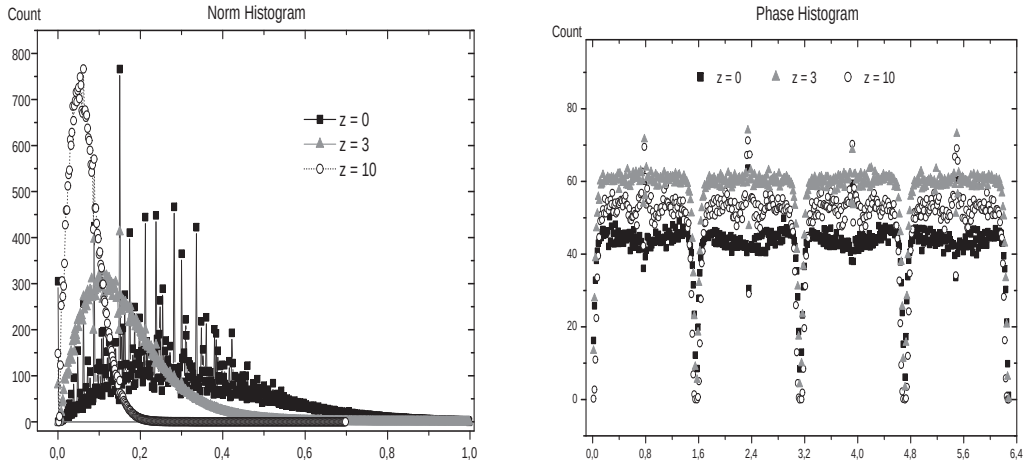

Fig. 3. Norms and phases histogram.

In Figure 3 we present the histogram of norms and phases of the gradient field. The statistical moments (mean, variance, skewness and kurtosis) of the norms and phases are plotted in Figures 4 and 5, respectively.

In Figure 3 we can observe the evolution of the norms and phase histogram, as the system evolutes and the structure starts to collapse. It is evident on the histograms that the statistical distributions of norms is evolving to a higher asymmetrical distribution. As indicated by all the statistical moments for the norms estimated in Figure 4. This behavior is a strong evidence of an increase of amplitude fluctuations (i.e. inhomogeneity) in the density field. The distortion that happens on the norm distribution is characterized by an increase of mean, variance and skewness. However, in the kurtosis parameter, we can observe that the redshift $z \sim 3$ is a crucial point in the norm distribution, since the kurtosis start to decrease after this point. At $z \sim 3$, another change in the norm distribution can be observed, the increase rate in the skewness parameter is lower after this point.

The distortions in the phase distribution are not so well defined as the case of the norms, since there are too much statistical fluctuations, as can be observed in Figure 5. It is difficult to conclude any evidence of anisotropy, however, the phase distribution reveals a higher dispersion and a decrease in the mean phase for redshift lower than $z \sim 3$. The phase variations have small amplitude, but it is possible to infer a considerable increase in phase variance, and kurtosis, specially for redshift lower than 3, while the mean increases at the beginning of the clustering process and start to decline for lower redshifts. Again, the time scale of $z \sim 3$ seems to play a special hole in the process of cosmic structure formation.

The interesting behavior of norm and phase distributions for low redshift can

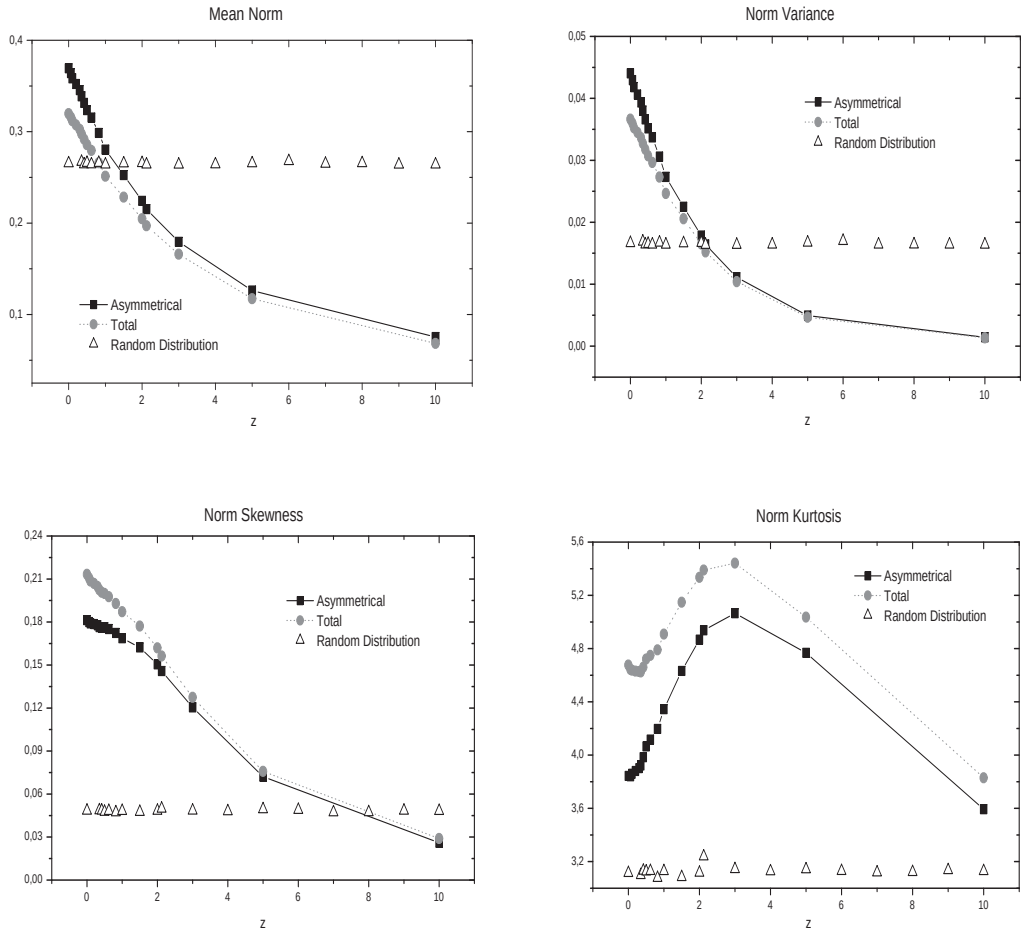

Fig. 4. Means, variance, skewness and kurtosis of the norms.

be observed by another feature of the GPA analysis, the number of gradient vectors in the density field. In figure 6, we show the total number of gradient vectors and the relative number of asymmetrical vectors. In this plot we can observe that the total number of vectors is increasing at the beginning of the clustering process at $z \leq 10$, has a maximum point at $z \sim 3$ and start to decline meaningfully for $z < 3$. Not only the total number of vectors is decreasing, but the relative number of asymmetrical vectors has a much more stronger decline. At $z \sim 3$ the asymmetrical vectors number is more than 80% of the field, while in present time, it is nearly 60%, less than it was at the beginning of clustering process $\sim 70\%$.

This result is an evidence that, for redshift lower than $z \sim (2-3)$, the local fluctuations in scales of $\sim 0.7 Mpc\ h^{-1}$ is getting smoothed. This feature can be explained by the infalling of matter in dynamically young galaxy clusters in conjunction with the formation of voids in the surroundings of overdensed regions. This feature is also indicated by the faster increase of the amplitude

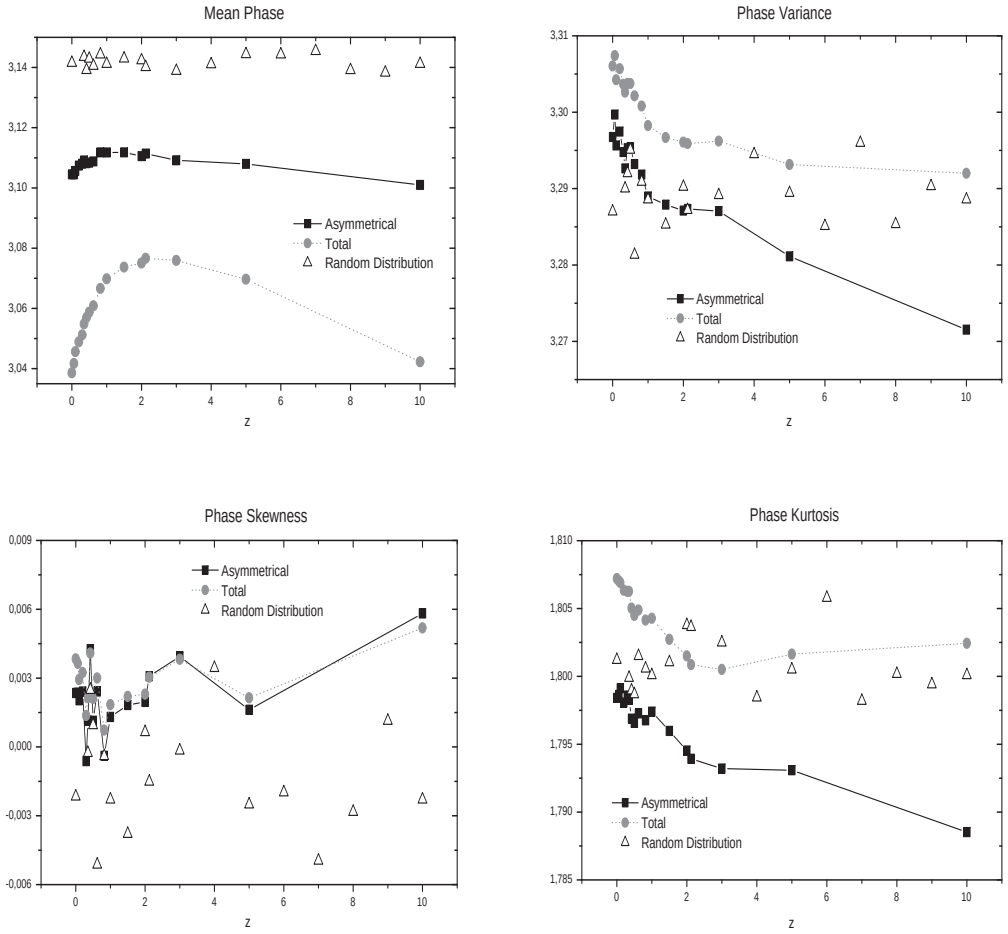

Fig. 5. Means, variance, skewness and kurtosis of the phases.

fluctuations (i.e. the mean vectors norm), at the same time, the underdensed regions are expanding, becoming large voids, where the gradient established is far below the mean value, or even null.

Comparing curves in Figures 4 and 5, it is possible to conclude that the field of asymmetrical vectors is also a good representation of the behavior of the gradient field, since the curves for total and the asymmetrical number of vectors present nearly the same behavior. However, the total number of vectors is indeed a better statistical assembly. Anyway, the investigation of the number of the asymmetrical vectors can bring additional information about symmetry breaking in the evolutionary process. Another point important to observe is that, as evidenced by the statistical analysis, the behavior of the pattern evolution of density fluctuations field is quite different from a pure random field. Indeed, the effects of time evolution is easily differentiable from a random case, specially for lower redshifts.

To better understand the evolution of the gradient pattern for the density field,

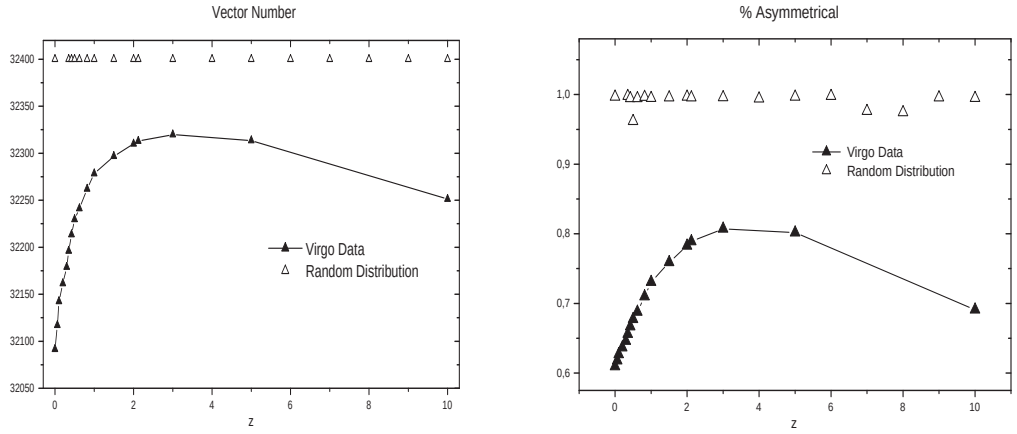

Fig. 6. The vectors number and the relative number of asymmetrical vectors.

z	Gauss	Lorentz	Log-Normal
0.0	0.45856	0.46068	0.48097
0.5	0.72328	0.72955	0.75061
1.0	0.85986	0.86963	0.88910
3.0	0.95181	0.95854	0.96624
5.0	0.96835	0.96865	0.96975
10.0	0.98180	0.97142	0.96782

Table 1
The correlation coefficient for the Gaussian, Lorentz and Log-Normal fit over the norm histogram.

we have performed a nonlinear curve fit to the norm histogram. The best fit parameters were obtained for three classes of curves: Gaussian, Lorentzian and Log-Normal. The correlation coefficient for some redshift values are showed in Table 1 below. In this table we can observe that for a redshift $z \sim 10$ the best fit is a Gaussian distribution, which characterizes a low correlated field. While the field evolves and the structures start to organize inside clusters after $z \leq 3$, the best fit is a Log-Normal distribution, which characterizes a higher correlated and asymmetrical field. This result illustrates the same behavior observed by the statistical moment analysis for the gradient field, specially the complex correlations illustrated in Figure 7 below.

An additional estimate to do with the gradient vectors field is the complex correlation between pairs of vectors, as defined in section 2.1. This parameter estimate may be helpful to elucidate how effective are the couplings in the global gradient field and their temporal relation. Accordingly, we would like to compare the GPA complex correlation with another correlation factor able

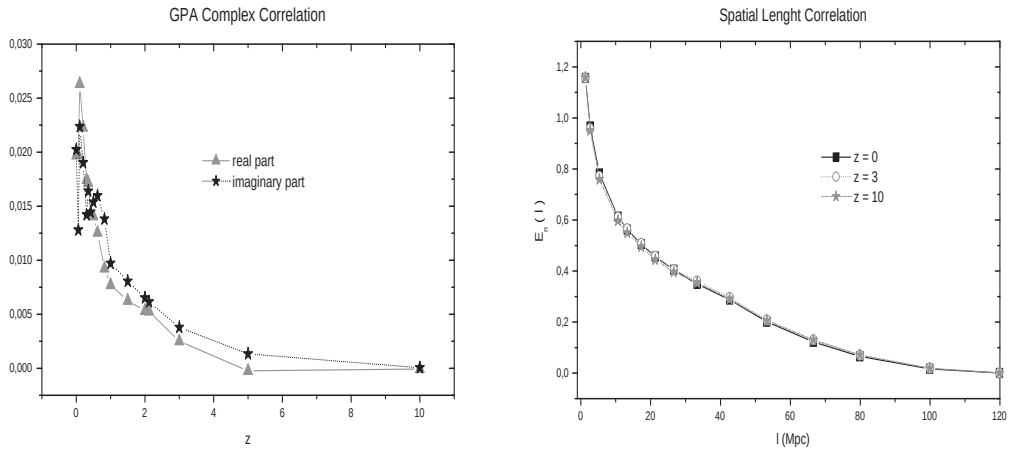

Fig. 7. The complex GPA correlation and the spatial length correlation.

to characterize spatial randomness by analyzing the properties of the field at different times, such as the spatial length correlation function, E_n (Cross & Hohenberg, 1993) :

$$En(l,t) \equiv \frac{\frac{1}{N}\sum_{i,j=1}^{N} \bar{x}(t)_n^{(i,j)} \bar{x}(t)_n^{(i+l,j+l)}}{\frac{1}{N}\sum_{i,j=1}^{N} (\bar{x}(t)_n^{(i,j)})^2}, \tag{1}$$

being: $\bar{x}(t)_n^{(i,j)} \equiv x(t)_n^{(i,j)} - \langle x \rangle_n$, where $x(t)_n^{(i,j)}$ is the amplitude matrix in (i,j) position, in a time scale t, and l is the spatial displacement ($l = 1, 2...$). The $E_n(l)$ function can be used as a rough quantitative measure of correlations for a given spatial profile in a fixed time scale, t.

The estimate for the GPA complex correlation and the $E_n(l)$ correlation function for z=10, 3 and 0 are illustrated in Figure 7. Both correlation factors represent simple statistic factors, but have completely different concepts: the former is a global statistic applied in the local fluctuations, while the second is a straight measure of spatial correlations in the amplitude field. The decaying behavior of the spatial correlation function in coupled lattices presents a typical power-law decay, however, we can observe that the $E_n(l)$ function is unable to predict any temporal relation of the density field, in despite of the GPA complex correlation that, although it does not concern about spatial correlations in large scales, it is able to describe the temporal evolution of gradient correlations for the density field in scales of $0.7 Mpc\ h^{-1}$.

4 Discussion

The late stages of cosmic structure formation are usually modeled by discrete numerical simulations, which do not allow us to follow the details of the entire gravitational collective phenomena behind the structure growth. However, charactering the spatio-temporal evolution of matter clustering is an important task in cosmology, since we need to compare theoretical predictions with observational data. In this paper we present the first test of the gradient pattern analysis as an alternative tool to investigate and characterize the nonlinear growth of large scale structure in the Universe. In particular, we are checking the ability of the GPA second and third gradient moment to describe the pattern evolution in matter clustering.

We have performed the statistical analysis of the norm and phase for the gradient vectors estimated over the density fluctuations field for some bi-dimensional slices of the Universe. The results show that the GPA technique is able to discriminate pattern formation and evolution in large scale structures. As could be expected, the mean, variance and skewness of norms present an increase distribution distortion as the system evolutes and the fluctuations interact in a nonlinear way and the structures start to organize and to collapse in clusters and filaments. For the vectors phases, the statistical fluctuations are bigger, however the variance and kurtosis are well defined, and show, except for the mean values, a sensible distortion in time evolution, as it was expected for the process of structure clustering. The distortions in norms and phase distributions can be interpreted as an evidence of higher irregularities in the fluctuations field for the scale investigated, $0.7 Mpc\ h^{-1}$. The GPA complex correlation is well defined and corresponds to the increase of amplitude fluctuations and phase interactions as the density field evolutes and the statistical behavior starts to differentiate from a random field, as observed on the best fit distribution over the norms histogram.

Nevertheless, the most important result of this first GPA investigation on N-body cosmological simulations seems to be the *turned point* observed in the number of asymmetrical vectors in the gradient field for $z \leq 3$. This epoch probably marks an intensification of galaxy cluster formation with substructures organizing inside clusters. This result suggests the application of the GPA statistical analysis for simulations in different scales, in order to have a better resolution to map substructures in galaxy clusters, as well as large patterns like wall filaments and voids regions.

Anyway, the decline in the number of gradient vectors may be directly related to the expansion of interlocked empty spaces between structures inside the galaxy clusters or even with the expansion of large empty structures, like big voids, which have a spherical expanding feature and can reach sizes up to

tens of Mpc (Sheth & Weygaert, 2004). The redshift $z \sim 3$ may represent the time scale of the voids structures building, however, to assure this conclusion it is necessary a detailed investigation in different scales and resolution. We hope that future works with the GPA technique may bring some additional information about the size, the spatial correlation and time evolution of voids.

In this first test, we may conclude that the statistical analysis of the second and third gradient moment may be useful to describe pattern evolution in a nonlinear interactive field. This result is very stimulating for future investigations of the gradient pattern formation analysis in the process of cosmic structure formation. At this moment, we are applying the gradient analysis over the DPOSS observational data for galaxy and cluster distribution, in order to compare with the temporal evolution characterized for a simulated Λ-CDM Universe. The next step on the GPA investigation on cosmic structure formation will be to perform the same statistical analysis of the second and third gradient moments in different scales, trying to estimate the asymmetrical fragmentation of gradient field with the help of the Delaunay triangulation process. We are also planning to expand this calculation to a three-dimensional mesh.

Acknowledgments

Special thanks to *Virgo Consortium* team. APAA thanks the financial support of CNPq and FAPESB, under grant 1431030005400. ALBR thanks the financial support of CNPq, under grant 470185/2003-1 and 306843/2004-8.

References

[1] Bardeen J.M. et al., 1986, ApJ, 304, 15.

[2] Bernardeau F., Weygaert R., 1996, MNRAS, 279, 693.

[3] Chiang LY., Coles P., Naselsky P.D., 2002, MNRAS, 337, 488.

[4] Cross M.C., Hohenberg P.C., 1993, Rev. Mod. Phy., 65, 851.

[5] Jenkins A. et al., 1998, ApJ, 499, 20.

[6] Martinez V. & Saar E., 2002, Statistics of the Galaxy distribution, Chapman & Hall/CRC, Boca Raton FL.

[7] Mecke K.R., Buchert T., Wagner H., 1994, A&A, 288, 697.

[8] Ramos F.M. et al., 2000, Physica A, 283, 171.

[9] Rosa R.R., Sharma A.S., Valdivia J.A, 1999, Int. J. Mod. Phys. C, 10, 147.

[10] Rosa R.R. et al., 2003, Brazillian J. Phys., 33, 605.

[11] Rosa R.R. et al., 2006, in preparation.

[12] Sheth R.K., Weygaert R., 2004, MNRAS, 350, 517.

[13] Springel V. et al., 2005, Nature, 535, 629.

[14] Weygaert R., 2002, Proceedings 2nd Hellenic Cosmology Workshop, Eds. M. Plionis, S. Cotsakis, I. Georgantopoulos, Kluwer.